Journal of Thermal Analysis and Calorimetry (2019) 138:3039–3054
https://doi.org/10.1007/s10973-019-08326-1

Albendazole-cyclodextrins binary systems

Thermal and spectral investigation on drug-excipient interaction

Cristina Trandafirescu[1] · Ionuţ Ledeţi[1] · Codruţa Şoica[1] · Adriana Ledeţi[1] · Gabriela Vlase[2] · Florin Borcan[1] · Cristina Dehelean[1] · Dorina Coricovac[1] · Roxana Racoviceanu[1] · Zoltán Aigner[3]

Received: 5 November 2018 / Accepted: 27 April 2019 / Published online: 15 May 2019

Abstract
The aim of this study was to characterize the interaction between the binary systems of albendazole (ABZ)—cyclodextrins (CDs) with pharmaceutical excipients. Hydroxyl-propyl-beta-cyclodextrin (HPBCD) and random methyl-beta-cyclodextrin (RAMEB) were used as cyclodextrins and magnesium stearate, mannitol, polyvinylpyrrolidone K30 (PVP K30), colloidal silica, starch, and talc were used as excipients. The utilized investigation techniques were attenuated total reflection Fourier transform infrared spectroscopy (ATR-FTIR), powder X-ray diffractometry (PXRD) and thermoanalytical techniques: thermogravimetry (TG)/derivative thermogravimetry (DTG)/heat flow (HF) and differential scanning calorimetry (DSC). The ATR-FTIR analysis clearly suggested interactions under ambient conditions between ABZ-HPBCD with PVP K30 and SiO_2 and between ABZ-RAMEB with SiO_2 and talc. The PXRD patterns indicated the formation of less crystalline mixtures but with no clear indication of interactions, since no peaks appeared nor disappeared. The modifications on the DSC curves suggested an interaction between ABZ-HPBCD and PVP K30 and SiO_2 respectively, and in case of ABZ-RAMEB was observed an interaction with talc. Thermal analysis (TG/DTG/HF) carried out in open crucibles in dynamic air atmosphere suggested that at temperatures over 40 °C dehydration of samples occurred, later followed by thermolysis and appearance of interactions in all studied cases. Our study concludes by recommending precautionary measures in elaborating new solid formulations containing ABZ, HPBCD and PVP K30/SiO_2 and for the ones containing ABZ, RAMEB and Talc/SiO_2, due to the present interactions under ambient conditions.

Keywords Albendazole · Cyclodextrins · Pharmaceutical excipients · Compatibility study

Cristina Trandafirescu and Ionuţ Ledeţi have contributed equally to the work.

✉ Codruţa Şoica
codrutasoica@umft.ro

Cristina Trandafirescu
trandafirescu.cristina@umft.ro

Ionuţ Ledeţi
ionut.ledeti@umft.ro

Adriana Ledeţi
afulias@umft.ro

Gabriela Vlase
gabriela.vlase@e-uvt.ro

Florin Borcan
fborcan@umft.ro

Cristina Dehelean
cadehelean@umft.ro

Dorina Coricovac
dorinacoricovac@umft.ro

Roxana Racoviceanu
babuta.roxana@umft.ro

Zoltán Aigner
aigner@pharm.u-szeged.hu

Extended author information available on the last page of the article

Introduction

Albendazole (ABZ, Fig. 1) is one of the most effective broad-spectrum anthelminthic drugs, used to treat intestinal and systemic helminth infections. Moreover, it is one of the few agents active against *Giardia lamblia* infections [1–3].

Albendazole has a very low aqueous solubility (0.01 mg mL^{-1} in water at 25 °C) and a high permeability through the biological membranes. Albendazole is characterized by a slow dissolution rate, a poor absorption from the gastro-intestinal tract, resulting in insufficient and erratic oral bioavailability. The low water solubility of ABZ is a major drawback in obtaining an optimal therapeutic response and also reduces the alternatives in drug formulations [4, 5].

One of the strategies used to overcome poor drug water solubility is complexation with cyclodextrins (CDs) [6, 7]. Cyclodextrins are now considered valuable pharmaceutical excipients used to improve drug bioavailability, to enhance drug stability and *to prevent drug-excipient interactions* [8–11]. In our previous work, we obtained supramolecular complexes of ABZ with hydroxy-propyl-beta-cyclodextrin (HPBCD) and methylated beta-cyclodextrin (RAMEB) which showed improved water solubility and dissolution rate in physiological simulated fluids [12–14]. The choice of the two semisynthetic cyclodextrin derivatives over the native β-cyclodextrin (BCD) as host molecules for albendazole was based upon their significantly higher aqueous solubility compared to their parent analogue; due to this increased water solubility, the semisynthetic derivatives are able to carry a higher amount of albendazole in solution compared to the native BCD. Currently, due to their low toxicity, most BCD derivatives are accepted by the European Medical Agency (EMA) as pharmaceutical ingredients for all administration routes except the parenteral one where only two derivatives, including HPBCD, are approved [15].

Previous molecular docking studies (unpublished) have shown that the albendazole molecule is partially included in the cavity of the host cyclodextrin, more specifically through its benzene moiety; the carboxamide functional group remains outside of the cyclodextrin cavity.

The rational design of novel pharmaceutical formulations requires very rigorous examination of the possible interactions between an active pharmaceutical ingredient (API) and excipients, as an essential part of the preformulation studies.

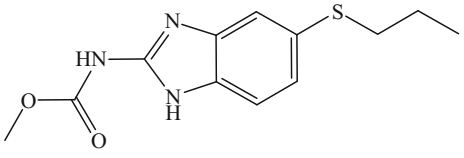

Fig. 1 Structural formula of albendazole

Having in mind the improvement of the bioavailability of ABZ, we extended the research in order to identify suitable excipients that could be used in solid pharmaceutical formulations of albendazole. Consequently, the aim of this study is to investigate the compatibility of six pharmaceutical excipients with ABZ–HPBCD and ABZ-RAMEB inclusion complexes. This study also offers a better understanding of solid–solid interaction in multicomponent systems, giving valuable information for the rational design of novel solid pharmaceutical formulations of ABZ.

The selected excipients were magnesium stearate, mannitol, polyvinylpyrrolidone PVP K30, colloidal silica, starch, and talc.

Materials and methods

Materials and sample preparation

Albendazole (methyl [5-(propylsulfanyl)-1*H*-benzimidazol-2yl]carbamate) was obtained from Biesterfeld, Hamburg, Germany (pharmaceutical grade) and used as received.

The tested pharmaceutical excipients (pharmaceutical grade) were used as received: magnesium stearate (Fluka, Germany), mannitol (Merck, Germany), polyvinylpyrrolidone PVP K30 (Sigma-Aldrich, Germany), colloidal silica (Aerosil 200Evonik Degussa, Germany), starch (Grain Processing Corporation, USA), talc (Luzenac Pharma, Italy). Hydroxyl-propyl-beta-cyclodextrin (CY-2005.2) and methylated beta-cyclodextrin (CY-2004.1) were purchased from Cyclolab, Budapest, Hungary.

Albendazole-cyclodextrin complexes were prepared in 1:1 molar ratio using the kneading method; briefly, precise amounts of ABZ and HPBCD or RAMEB, respectively, were pulverized in a ceramic mortar and carefully mixed into a physical mixture. A mixture of ethanol–water (1:1, w/w), in equal amount with the previously obtained physical mixture of individual compounds, was added under continuous kneading until the evaporation of the bulk solvent. After drying at room temperature for 24 h, the products were dried in the oven at 105 °C, until constant mass. The final products were pulverized and sieved [12] giving a yield of 95%. The stoichiometry of the final complexes was previously determined by the authors by conducting phase-solubility studies according to the Higuchi and Connors method [14]; briefly, an excess of active substance, albendazole, was added to various concentrations of HPBCD and RAMEB, respectively, and the suspensions were shaken at room temperature for 7 days until reaching equilibrium. The concentration of the dissolved drug was spectrophotometrically assessed in the supernatant and the solubility diagram was built. According to the literature [6, 14], the A_L type of the solubility

diagram together with its subunitary slope value reflect the formation of a 1:1 binary complex.

The physical mixtures between the ABZ-CDs complexes and the selected excipients were obtained by dry kneading of the components in agate mortar for at least 5 min. All the prepared samples were kept in glass vials in order to be submitted to the analysis.

The interaction study was performed using physical mixtures of ABZ-HPBCD/ABZ-RAMEB and excipients of equal masses (1:1). The mass ratio of 1:1 (drug:excipient) was chosen in order to maximize the probability of observing the interactions [16].

Instrumental techniques

The most frequently used analytical techniques for compatibility screening studies are thermal methods and spectroscopic methods [17–23]. For this purpose, attenuated total reflection Fourier transform infrared spectroscopy, X-ray powder diffraction and thermal analysis (TG/DTG and DSC) were used.

ATR-FTIR spectroscopy

Attenuated Total Reflection Fourier Transform Infrared Spectroscopy spectra of the samples were recorded on a Perkin Elmer SPECTRUM 100 device. Spectra were collected in the 4000–650 cm^{-1} spectral range, with a resolution of 1 cm^{-1} and with 32 co-added scans.

Powder X-ray powder diffraction

The PXRD experiments were performed with a Bruker D8 Advance diffractometer (Bruker AXS GmbH, Karlsruhe, Germany) using the symmetrical reflection mode with Cu Ka radiation (λ = 1.5406 Å) and Göbel Mirror bent gradient multilayer optics. Scattered intensities were measured with a Våntec-1 line detector. The angular range included 3°–50° in steps of 0.01°. Other relevant measurement conditions were as follows: target, Cu; filter, Ni; voltage, 40 kV; current, 40 mA; measuring time, 0.1 s/steps.

Differential scanning calorimetry

The DSC curves were obtained using a Mettler-Toledo DSC1 instrument (Mettler Inc., Schwerzenbach, Switzerland); data analysis was performed using the STAR^e Thermal Analysis Software SW 12.10.

For each sample, approximately 2–5 mg were used (ABZ-HPBCD and ABZ-RAMEB complexes, each excipient and every binary mixture, respectively). The analysis was carried out in sealed aluminum crucible with pierced caps, by heating in the temperature range between 25 and 300 °C, with a heating rate of 5 °C min^{-1} in dynamic nitrogen atmosphere at a flow rate of 10 L h^{-1}. A reference material (empty aluminum crucible with pierced cap) simultaneously undergoes the same programmed time–temperature routine.

Thermoanalytical investigations

The thermoanalytical TG-thermogravimetry/DTG-derivative thermogravimetry/HF-heat flow curves were drawn up in an air atmosphere and under non-isothermal conditions at a heating rate of 10 °C min^{-1} using a Perkin-Elmer DIAMOND equipment. Samples of masses of approx. 6 mg were put into aluminum crucibles and heated by increasing temperature from ambient up to 500 °C. For determining the thermal effects, the DTA data (μV) were converted in HF (Heat Flow) data (mW).

Results and discussion

Excipients exert an important role in drug development, giving significant advantages to medication. They have a substantial role in bioavailability, improving drug solubility, stability, and permeability [24]. Although excipients are considered pharmacologically inert, they may initiate, propagate or participate in physical and/or chemical interactions with an API, compromising the effectiveness of the medication [25, 26].

It is well known that in a solid pharmaceutical formulation, the main objective is to maintain the integrity of the active ingredient in terms of both structure and concentration. Since the interactions occur between "reactive" functional groups of the API and the ones of excipients, solely the information regarding the API are interpreted during the instrumental investigations. Following these considerations, by all investigational tools, the modification of the characteristic signals (FTIR bands, PXR peaks, thermal events) of the complexes vs. binary mixtures were investigated.

Initially, the compatibility studies were performed under ambient temperatures, using ATR-FTIR spectroscopy and PXRD and later the samples were subjected to thermal stress (TG/DTG/HF simultaneous analysis and DSC), in order to evaluate the thermal-induced interactions between the components.

ATR-FTIR spectroscopy

ATR-FTIR spectra recorded in the spectral range 4000–650 cm^{-1} are presented in Figs. 2 and 3. The data were presented comparatively for each inclusion complex (ABZ-HPBCD and ABZ-RAMEB, respectively) with the binary mixture of each excipient.

Spectroscopic methods are used to obtain accurate and concise data about possible interactions between an API

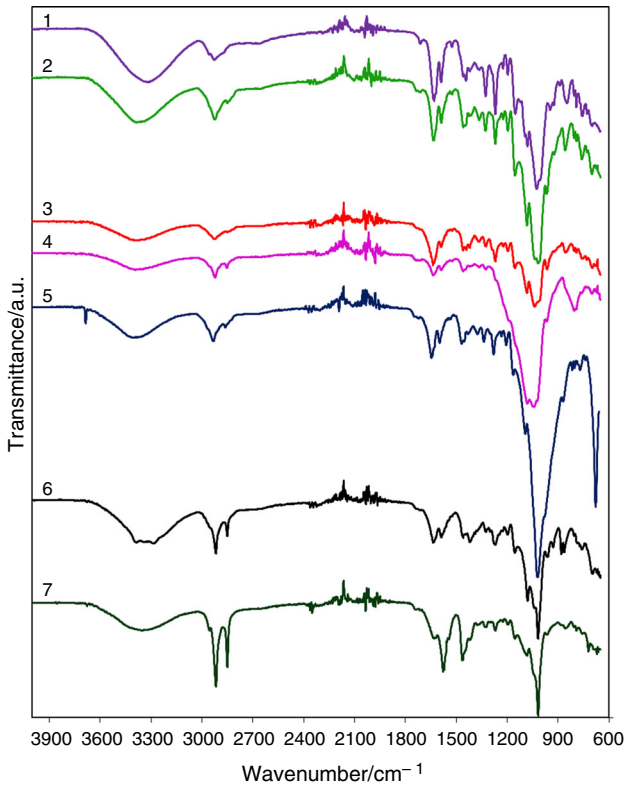

Fig. 2 ATR-FTIR spectra recorded for: 1. ABZ-HPBCD; 2. ABZ-HPBCD + Sta; 3. ABZ-HPBCD + PVP; 4. ABZ-HPBCD + SiO_2; 5. ABZ-HPBCD + Talc; 6. ABZ-HPBCD + Man; 7. ABZ-HPBCD + MgSt

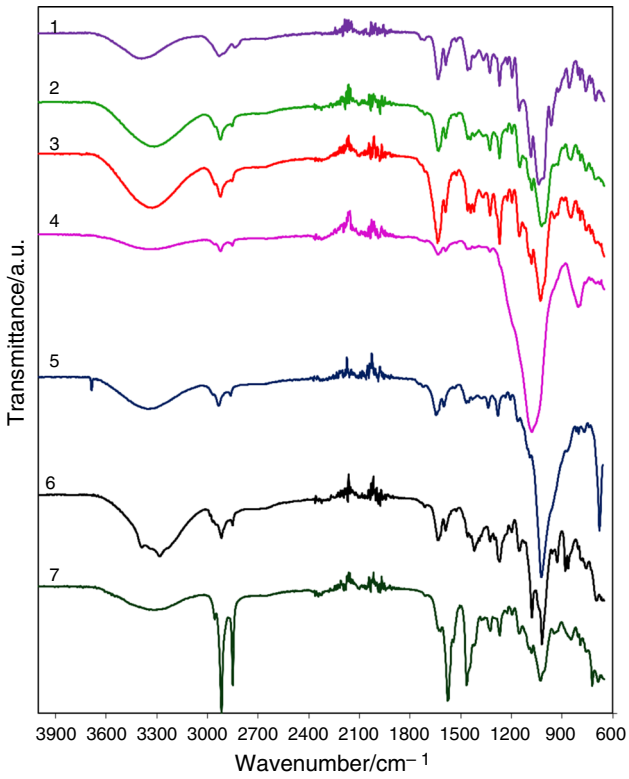

Fig. 3 ATR-FTIR spectra recorded for: 1. ABZ-RAMEB; 2. ABZ-RAMEB + Sta; 3. ABZ-RAMEB + PVP; 4. ABZ-RAMEB + SiO_2; 5. ABZ-RAMEB + Talc; 6. ABZ-RAMEB + Man; 7. ABZ-RAMEB + MgSt

and excipients [17, 20–22]. The superiority of ATR spectroscopy vs. classic salt pelleting method resides in the fact that no interactions or modifications of components are due to sample preparation, mainly the intense grinding and applied pressure [27, 28]. In ATR-FTIR spectroscopy, the vibrational changes observed in the spectrum of API-excipient physical mixture, highlight potential intermolecular interaction between the components [27–31].

For the ABZ-HPBCD, the FTIR spectrum shows several characteristic bands, as follows: between 3680 and 3012 cm^{-1} a broad band is observed, due to the presence of water (peak at 3327 cm^{-1}) and weak bands due to characteristic C–H stretching vibrations for CH_3 and CH_2 groups from the propyl moiety of ABZ, in the 3000–2840 spectral range (peaks at 2958, 2931 and 2869 cm^{-1}). The presence of the C–H stretching vibrations for CH_3 and CH_2 groups from the propyl moiety of ABZ may suggest that this group is not completely inserted in the cyclodextrin moiety.

However, some of the characteristic bands of the ABZ are no longer visible in the spectrum of the complex, like the ones previously published by Trandafirescu et al. in 2016 [32]: the stretching of N–H amine (in the spectral range 3413–3188 cm^{-1}, peak at 3317 cm^{-1}), the aromatic benzoimidazolyl system (the band at 1618 cm^{-1}), or are shifted to different wavenumbers (like the benzoimidazolyl band from 1629 cm^{-1} in ABZ to 1635 cm^{-1} in complex). In the case of the ABZ-HPBCD complex, the bands appear at the same wavenumbers or shifted, in comparison to the ones reported for ABZ, as seen in Table 1. The attribution of the bands to functional groups is difficult, since the API is partially encapsulated in the cyclodextrin cavity.

However, through the analysis of the bands shown by the spectra of the binary mixtures, a more complex pattern can be noticed, due to the overlapping of the excipients bands. Some bands were drastically attenuated due to the presence of the bands of excipients, while some bands disappeared or were shifted to different wavenumbers. Interactions can be assumed solely in the case of ABZ-HPBCD with SiO_2 (several bands of the complex are no longer present, like the bands at 1443, 1224, 1197, 1153, 1004, 947, 846 and 757 cm^{-1}, respectively), as well as in the case of its mixture with PVP K30, as presented in Table 1.

Data from the literature describes the ability of PVP to interact with compounds containing hydrogen-donating functional groups due to its carbonyl group which is pivotal to degradation; moreover, PVP may contain peroxides as residue, responsible for the formation of oxides. The high moisture content of this excipient also enhances the possibility of hydrolysis of drugs [25, 33]. In our study, the disappearance of

Table 1 The ATR-FTIR bands observed for inclusion complexes of ABZ and in binary mixtures with selected excipients

Sample	Analysis of ATR-FTIR spectral regions/cm^{-1}		
	4000–2500	1800–1000	1000–400
ABZ [31]	3317; 2958; 2868; 2659	1712; 1629; 1618; 1587; 1525; 1440; 1419; 1325; 1265; 1222; 1193; 1120; 1095; 1058; 1006	958; 923; 887; 864; 806; 790; 771; 759; 729; 696; 611; 597; 511; 422
ABZ-HPBCD	3680–3012; 3327; 2958; 2931; 2869	1712; 1635; 1589; 1443; 1327; 1269; 1224; 1197; 1153; 1081; 1025; 1004	947; 846; 792; 757; 699
ABZ-HPBCD + MgSt	3650–3036; 3359; 2958; 2918; 2851	1630; 1577; 1571; 1463; 1459; 1323; 1269; 1225; 1197; 1157; 1084; 1018;	964; 792; 721; 671
ABZ-HPBCD + Man	3677–3027; 3385; 3285; 2985; 2957; 2919; 2851	1637; 1590; 1461; 1421; 1327; 1269; 1225; 1195; 1156; 1080; 1037; 1019;	963; 929; 882; 863; 698
ABZ-HPBCD + PVP K30	3645–3043; 3386; 2925; 2851	1638; 1631; 1590; 1460; 1442; 1421; 1367; 1327; 1270; 1224; 1197; 1154; 1082; 1040; 1019	966; 925; 857; 806; 792; 757; 699
ABZ-HPBCD + SiO_2	3680–3020; 3380; 2955; 2923; 2852	1713; 1637; 1631; 1590; 1459; 1328; 1269; 1082; 1044; 1022;	969; 805; 791; 694
ABZ-HPBCD + Sta	3674–3036; 3386; 2924; 2851; 2839	1712; 1637; 1631; 1589; 1459; 1452; 1443; 1421; 1365; 1328; 1270; 1224; 1197; 1154; 1083; 1038; 1017;	967; 923; 858; 806; 793; 760; 730; 699
ABZ-HPBCD + Talc	3700–3020; 3676; 3390; 2956; 2923; 2852;	1712; 1638; 1631; 1620; 1589; 1460; 1443; 1366; 1327; 1269; 1224; 1196; 1155; 1083; 1011;	861; 807; 792; 761; 730; 669
ABZ-RAMEB	3700–3035; 3389; 2931; 2839;	1734; 1716; 1637; 1632; 1589; 1525; 1459; 1451; 1443; 1365; 1328; 1270; 1223; 1197; 1155; 1084; 1039; 1007	965; 924; 857; 806; 792; 759; 730; 702;
ABZ-RAMEB + MgSt	3600–3006; 3338; 2958; 2916; 2851	1631; 1619; 1577; 1572; 1543; 1465; 1326; 1270; 1224; 1195; 1155; 1081; 1029; 1007;	924; 847; 807; 792; 758; 722; 685;
ABZ-RAMEB + Man	3700–3005; 3388; 3340; 3283; 2985; 2971; 2918; 2851	1712; 1637; 1631; 1589; 1525; 1460; 1420; 1327; 1302; 1270; 1198; 1154; 1079; 1018;	959; 928; 881; 863; 807; 785; 697
ABZ-RAMEB + PVP K30	3695–3015; 3327; 2957; 2923; 2855	1637; 1631; 1619; 1591; 1525; 1460; 1441; 1421; 1326; 1270; 1224; 1197; 1153; 1122; 1096; 1080; 1026; 1007	948; 925; 891; 845; 806; 792; 757; 731; 671
ABZ-RAMEB + SiO_2	3670–2990; 3349; 2960; 2922; 2851;	1637; 1631; 1589; 1525; 1460; 1420; 1327; 1302; 1270; 1198; 1154; 1076;	804; 792; 760; 731
ABZ-RAMEB + Sta	3680–3010; 3316; 2957; 2922; 2850;	1713; 1637; 1631; 1619; 1591; 1526; 1459; 1422; 1366; 1328; 1270; 1225; 1196; 1152; 1080; 1020; 1003	923; 847; 806; 792; 759; 729; 702
ABZ-RAMEB + Talc	3705–3005; 3677; 3345; 2956; 2924; 2853	1714; 1637; 1631; 1619; 1590; 1525; 1459; 1442; 1421; 1327; 1270; 1223; 1195; 1155; 1080; 1011	863; 806; 792; 759; 730; 669

several bands of the complex may be attributed to a chemical interaction between the ABZ and PVP K30.

Colloidal silica has a large specific surface due to its small particle size, giving high adsorption properties. The excipient also may act as a Lewis acid under anhydrous conditions and promote reactions as hydrolysis, transesterifications and cyclisations, as well as physical events as epimerizations and dehydrations [33]. Hence, we may presume that an interaction between ABZ and colloidal silica took place under experimental conditions.

In the case of ABZ-RAMEB, ATR-FTIR suggested interactions with Talc and SiO_2, also sustained by the complete disappearance of some bands (Fig. 3 and Table 1). Data from the literature mentions that talc may form inorganic intercalation compound where hydrogen bonding being the major interaction between talc and the drug [34]. In case of ABZ-RAMEB, very probable, this kind of physical interaction took place. The type of interaction with SiO_2 we assumed that it is similar to that described above, for ABZ-HPBCD.

PXRD patterns

PXRD was employed as a second investigational tool for the evaluation of the compatibility between each inclusion complex and selected excipients under ambient condition. PXRD patterns of ABZ and physical binary mixtures were plotted as intensity (arbitrary units) *vs.* diffraction angle (2θ).

Powder X-ray diffractometry enables qualitative and quantitative determination of the crystallinity of an API in order to investigate the possible interaction between drug and excipients.

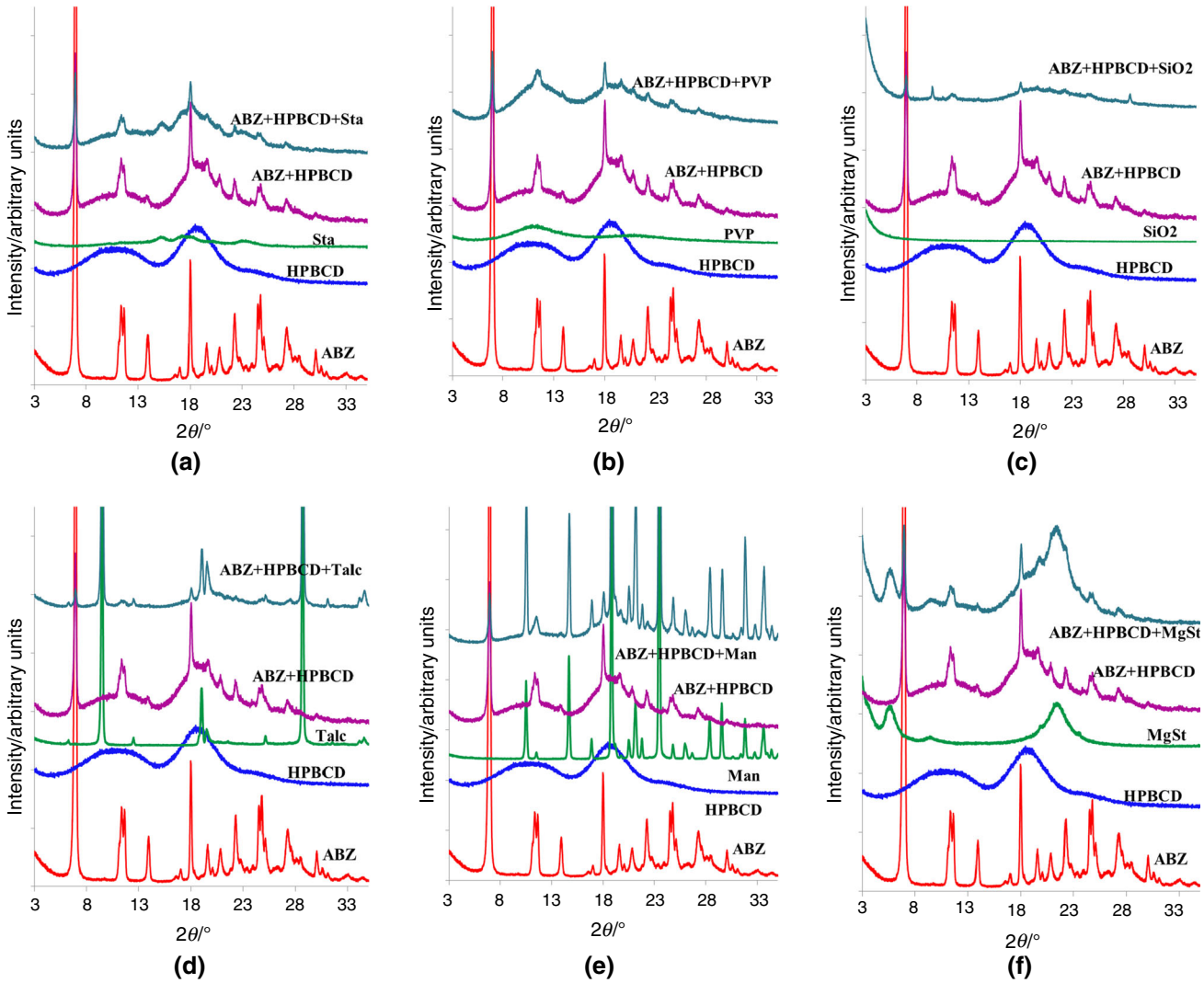

Fig. 4 PXRD patterns recorded for ABZ, HPBCD, ABZ-HPBCD inclusion complex and each excipient: **a** Sta, **b** PVP, **c** SiO_2, **d**Talc, **e** Man and **f** MgSt

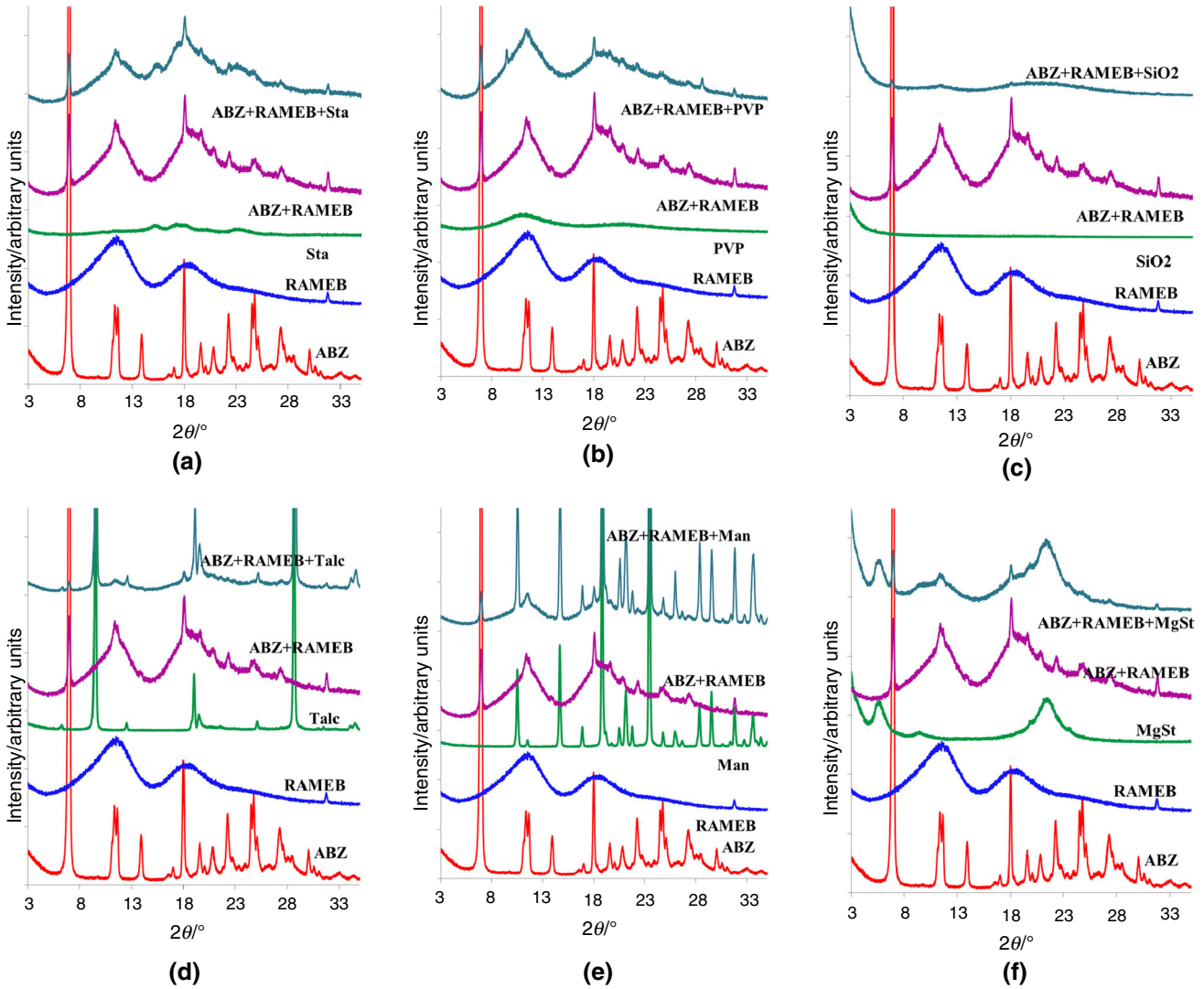

Fig. 5 PXRD patterns recorded for ABZ, RAMEB, ABZ-RAMEB inclusion complex and each excipient: **a** Sta, **b** PVP, **c** SiO_2, **d** Talc, **e** Man and **f** MgSt

Table 2 The PXRD pattern recorded for ABZ, ABZ-HPBCD and binary mixtures with selected excipients

ABZ	ABZ-HPBCD	ABZ-HPBCD+					
		Sta	PVP K30	SiO_2	Talc	Man	MsSt
6.85	6.84	6.91	6.90	6.90	6.88	6.86	6.94
11.31	11.32	11.15	11.16	11.01		11.35	11.28
11.36	11.41						
13.88	13.48						
17.97	17.98	17.94	17.96	17.94	17.96	17.99	18.01
19.51	19.25					19.46	19.55
20.75	20.68						
22.22	22.15	22.14	22.07			22.02	
24.49	24.46	24.46	25.10		25.10	24.77	24.52
27.20	27.07	27.09		28.52	28.83	27.08	27.07

Table 3 The PXRD pattern recorded for ABZ, ABZ-RAMEB and binary mixtures with selected excipients

ABZ	ABZ-RAMEB	ABZ-RAMEB+					
		Sta	PVP K30	SiO_2	Talc	Man	MsSt
6.85	6.95	6.93	6.92	6.45	6.64	6.88	6.94
11.31	11.30	11.27	11.28			11.27	11.19
11.36							
13.88							
17.97	18.00	17.99	17.98		17.98	17.94	17.94
19.51	19.39	19.51					
20.75	20.64						
22.22	22.19		22.14				
24.49	25.12						
27.20	27.19	27.08					

The results of PXRD analysis are presented in Figs. 4 and 5 and in Tables 2 and 3. According to PXRD patterns, ABZ shows several diffraction peaks indicating a crystalline nature of the solid sample, while both cyclodextrins (HPBCD and RAMEB) are totally amorphous substances, without characteristic peaks [14]. The ABZ complexes with selected CDs are semi-crystalline samples. According to the obtained data, Man and Talc are crystalline solids with characteristic peaks, whereas the other four excipients (MgSt, PVP K30, SiO_2 and Starch) are of amorphous nature: MgSt is characterized by some broad peaks, while PVP K30, SiO_2 and Starch are totally amorphous substances, without any peaks (Figs. 4 and 5).

The X-ray diffraction patterns of binary mixtures can be considered as a superposition of the X-ray patterns of ABZ-CD and excipients, thus demonstrating the absence of any interaction. The X-ray diffraction patterns revealed that the ABZ-HPBCD/ABZ-RAMEB physical characteristics were not affected by the addition of excipients.

Differential scanning calorimetry

The DSC curves of each inclusion complex and their binary mixtures with excipients are presented in Figs. 6 and 7.

The summarized DSC data like the onset temperature (T_{onset}), the peak temperature (T_{peak}), the offset temperature (T_{offset}), and the associated enthalpy of the process (ΔH) of ABZ-CD in various excipient mixtures are displayed in Tables 4 and 5.

Differential scanning calorimetry is known to be a rapid and accurate technique used to investigate possible incompatibilities between API and excipients, allowing for quick information about possible interactions [18, 19]. The DSC enables to point out the thermal transition and the morphological changes of API and of the mixtures of API with different excipients, [29, 32, 35, 36]. Thermoanalytical techniques (TG/DTG/HF) complete the information obtained from the DSC analysis, clarifying more concisely the appearance of drug-excipient interaction [22, 37, 38].

The detailed DSC analysis of ABZ, ABZ-HPBCD and ABZ-RAMEB, respectively, are described in our previous studies [12–14], as well as the thermal behavior of excipients [32]. According to these data, ABZ shows a very good thermal stability and does not contain any crystallization water, since the first noticeable thermal events occur in the 169–215 °C temperature range, with peaks at 198 °C and 203 °C (the latter due to melting) [32]. Our previous findings regarding the study of interaction of ABZ with the same six pharmaceutical excipients, using DSC analysis, revealed thermal induced interactions between ABZ and MgSt, Man, PVP K30 and SiO_2, respectively, whereas no interactions were revealed only in case of Sta and Talc [32]. These results motivated us to investigate the influence of cyclodextrins on the compatibility of ABZ with pharmaceutical excipients.

The inclusion complex of ABZ-HPBCD shows two endothermal events in inert atmosphere, the first corresponding to a dehydration, while the latter is due to the melting of ABZ from the complex structure. The DSC curves recorded for binary mixtures reveal the presence of an endothermal event around 198 °C (except for the ABZ-HPBCD + Man), confirming that at this temperature the mixture still contains ABZ. Most of DSC curves show the first process of dehydration that occurs at temperatures below 134 °C, for all mixtures, except for the one with Man. Similar observations can be drawn from the results reported in the case of ABZ-RAMEB mixtures with excipients.

The results obtained by DSC analysis must be interpreted by taking into consideration the characteristics of this method: the high temperature conditions and the absence of moisture [19, 38]. The DSC profiles of physical mixtures of ABZ-HPBCD with MgSt, Sta, and Talc are almost superimposable, indicating that no interactions occur under the experimental conditions. The thermal profile of ABZ-HPBCD + Man exhibited only the thermal event characteristic for mannitol, highlighting the possible role of mannitol as enhancer, in inclusion complex

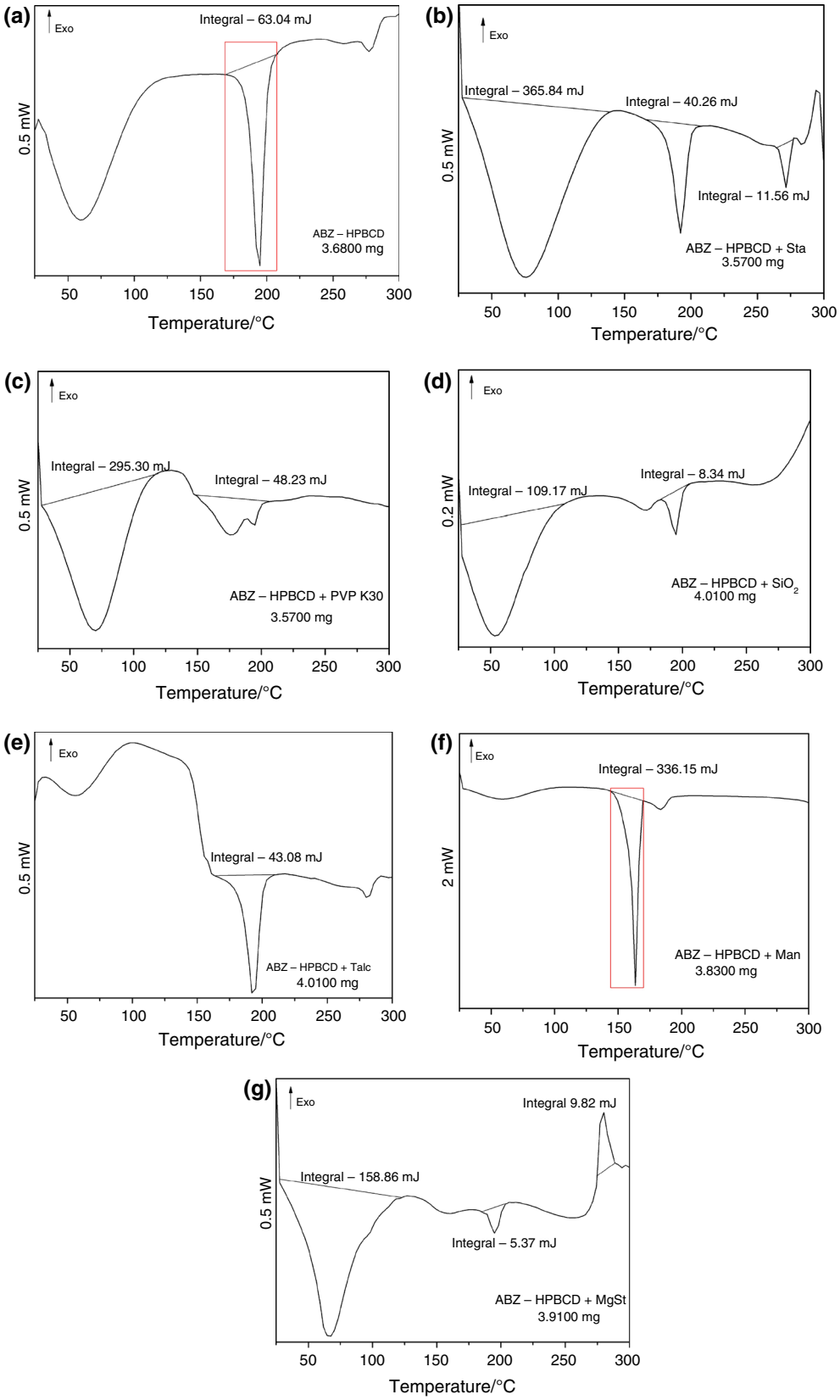

Fig. 6 DSC curves recorded for: **a** ABZ-HPBCD inclusion complex and for ABZ-HPBCD in mixture with: **b** Sta, **c** PVP, **d** SiO_2, **e** Talc, **f** Man and **g** MgSt

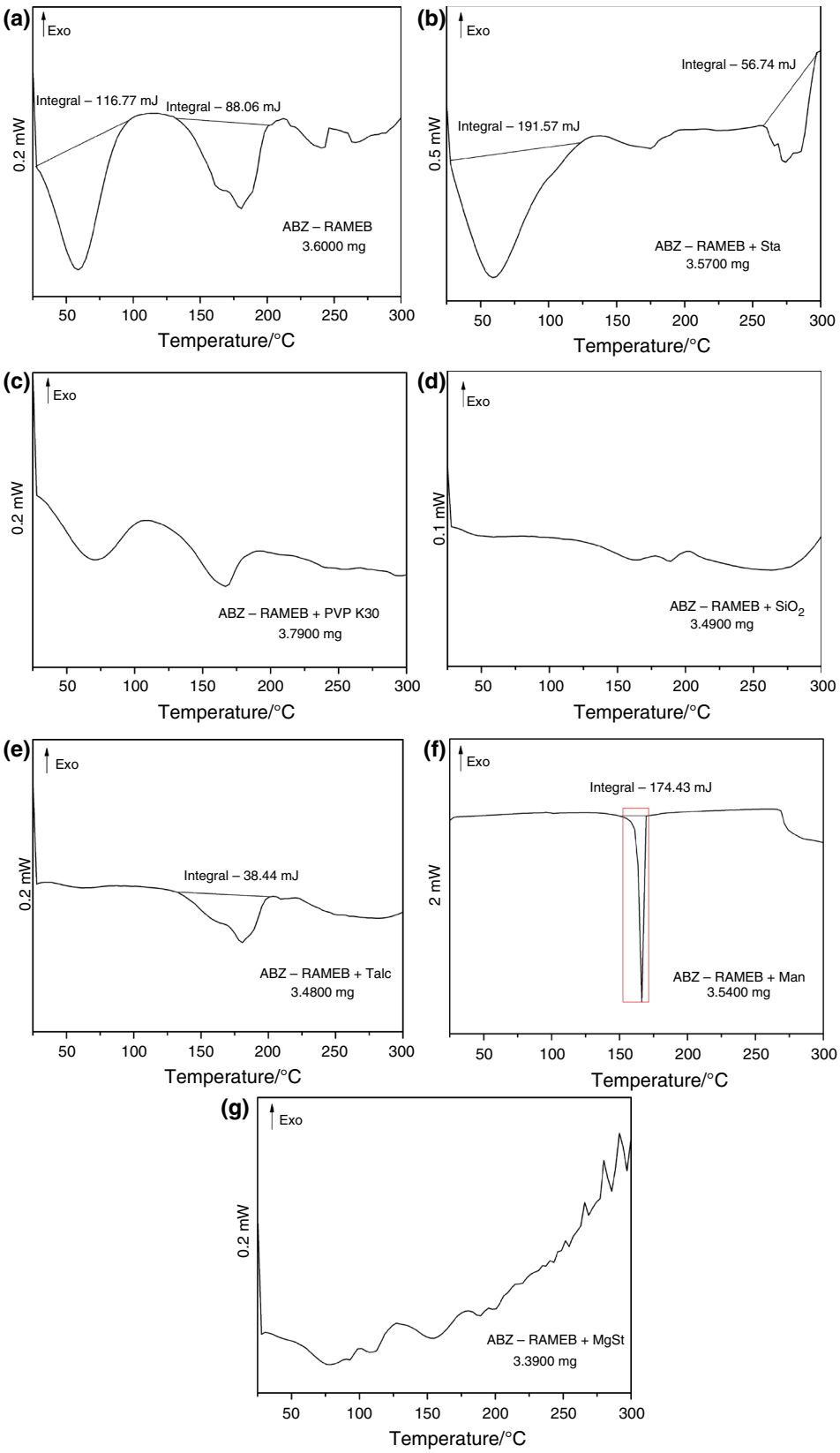

Fig. 7 DSC curves recorded for: **a** ABZ-RAMEB inclusion complex and for ABZ-RAMEB in mixture with: **b** Sta, **c** PVP, **d** SiO_2, **e** Talc, **f** Man and **g** MgSt

Table 4 The DSC data obtained for ABZ, ABZ-HPBCD and the physical mixtures with excipients

Sample	Thermal events revealed by the DSC curves				Interaction[a]
	T_{onset}/°C	T_{peak}/°C	T_{offset}/°C	ΔH/J g^{-1}	
ABZ	169	198, 203	215		
ABZ-HPBCD	25	61	119		
	173	194	210	–17.08	
ABZ-HPBCD + MgSt	28	65	119	–40.63	–
	188	195	204	–1.37	
	276	278	283	+2.51	
ABZ-HPBCD + Man	144	166	169	–87.76	–
ABZ-HPBCD + PVP K30	26	71	118	–82.72	+
	150	176, 197	203	–13.51	
ABZ-HPBCD + SiO_2	26	57	105	–27.23	+
	180	194	206	–2.08	
ABZ-HPBCD + Sta	25	76	134	–102.48	–
	177	192	204	–11.28	
	264	271	278	–3.24	
ABZ-HPBCD + Talc	25	57	98		–
	173	193	208	–10.74	

[a]Sign + signifies that interaction occurs, while − indicate that no interaction takes place

Table 5 The DSC data obtained for ABZ, ABZ-RAMEB and the physical mixtures with excipients

Sample	Thermal events revealed by the DSC curves				Interaction[a]
	T_{onset}/°C	T_{peak}/°C	T_{offset}/°C	ΔH/J g^{-1}	
ABZ	169	198, 203	215		
ABZ-RAMEB	25	59	93	− 29.11	
	134	161, 179	201	–21.96	
ABZ-RAMEB + MgSt	Not relevant				–
ABZ-RAMEB + Man	154	167	169	− 49.27	–
ABZ-RAMEB + PVP K30	25	69	110		–
	110	169	193		
ABZ-RAMEB + SiO_2	121	162	178		–
	178	188	204		
ABZ-RAMEB + St	25	59	122	− 53.66	–
	258	Multiple	296	− 15.89	
ABZ-RAMEB + Talc	133	180	199	− 11.05	+

[a]Sign + signifies that interaction occurs, while − indicate that no interaction takes place

formation. The thermal profiles of physical mixtures of ABZ-HPBCD with PVP K30 and SiO_2, respectively, exhibited a decrease in the value of the melting point of the ABZ-HPBCD complex, thus suggesting a possible incompatibility between the components. The observed thermal event, may be attributable to the interaction between the carbonyl group of PVP and ABZ.

The DSC findings on physical mixtures of ABZ-RAMEB and MgSt, Man, PVP K30, SiO_2 and Sta, respectively, revealed no thermal stress induced interaction; in case of the physical mixture with Talc, a decrease in the value of the melting peak was recorded, denoting a possible incompatibility. This interaction may be due to the formation of the inorganic intercalation compound between Talc and ABZ and/or to the presence of characteristic residues of talc: formaldehyde or heavy metals.

Following these considerations, more sensible techniques were used in order to evaluate the thermal induced interactions, such as TG/DTG/HF.

TG/DTG/HF

Initially, the thermoanalytical curves TG/DTG/HF were drawn up for the inclusion complexes, as shown in Fig. 8,

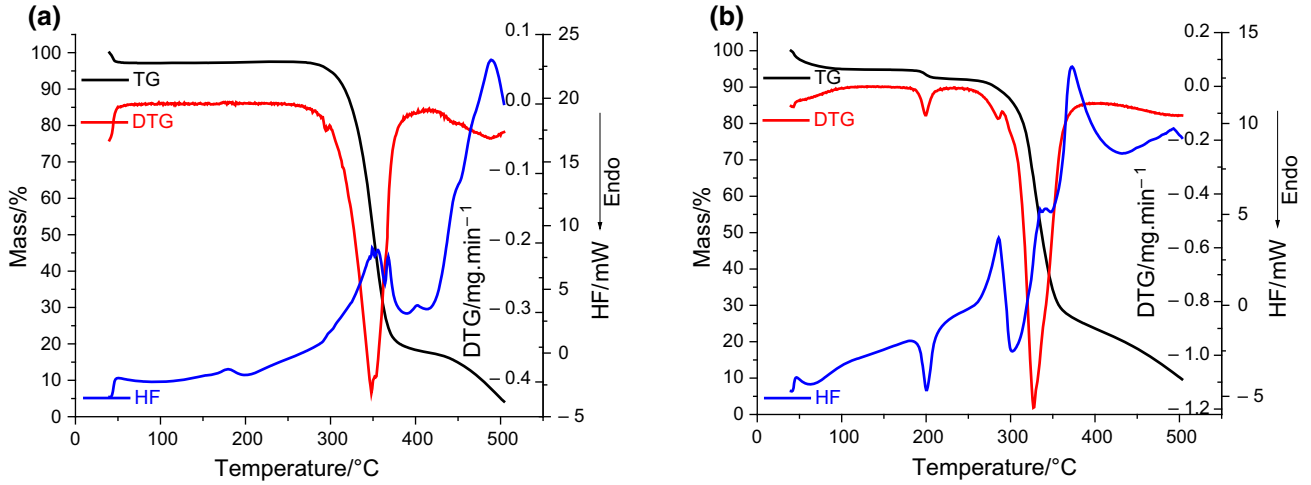

Fig. 8 Thermoanalytical curves obtained in air at 10 °C min^{-1} for: **a** ABZ-HPBCD and **b** ABZ-RAMEB

in order to determine the thermal stability and the main thermal events that took place during heating.

Following this, in similar conditions, the thermoanalytical data were recorded for all mixtures of inclusion complexes with the excipients, as shown in Fig. 9.

The thermoanalytical curves of the complex formed between ABZ and HPBCD show the thermal degradation in the following temperature ranges: 37–56 °C (with a mass loss determined by the presence of humidity Δm = 2.7%), 273–412 °C (Δm = 79.5%), and 412–500 °C (Δm = 13.67%). The first event noticed on the HF curve has a low intensity and an endothermic nature with a maximum at 181 °C corresponding to the melting process of the inclusion complex. The HF curve of this complex presents (Fig. 8a) a well-defined exothermic event split in two peaks (T_{peaks} at 351 and 369 °C) corresponding to the advanced thermolysis of the complex, later followed by another exothermic peak due to the final destruction of the structure, also confirmed by the thermogravimetrical curve. The DTG curve presents only one event with maximum at 347 °C (Fig. 8a).

The TG/DTG/HF curves of the complex between ABZ and RAMEB (Fig. 9) indicate that the thermal decompositions occur in five stages in the following temperature range: 42–95 °C (Δm = 4.6%), 172–223 °C (Δm = 2.3%), 247–300 °C (Δm = 5.6%), 300–385 °C (Δm = 61.3%) and 385–500 °C (Δm = 15.5%). The HF curve of the binary system ABZ-RAMEB exhibits two endothermic events with maximum at 82 °C (event corresponding to the dehydration process of the used cyclodextrin) and at 199 °C due to the melting process of the binary-system (these temperature values are different compared to the ones corresponding to the active substance ABZ with melting at 210 °C (Albendazole, on PubChem) or to the cyclodextrin which melts at 180 °C (RAMEB, on ChemSrc) respectively [39, 40]. Another three events present on the HF curve have exothermic nature with maximum at 284, 333 and 372 °C, respectively, representing the decomposition of the ABZ-RAMEB. The shift toward a lower temperature of the endothermic melting peak of ABZ observed in the HF curve of the analysed binary systems indicates a molecular interaction between the host (cyclodextrin) and the guest (ABZ) due to the formation of the inclusion complex. However, in order to have an in-depth perspective over the stability of ABZ during guest–host inclusion complexation and the excipient effect, in future studies we will analyse the decomposition mechanism of each pure complex *vs.* complex in mixture with pharmaceutical excipients, by tools of kinetic analysis [41–45].

In the case of ABZ-HPBCD mixtures with various excipients, the analysis of TG/DTG curves (Fig. 9a, c) shows that the mass loss process occurs in the same interval range as for the complex alone. All samples show a mass loss below 50 °C, due to dehydration, followed by a good thermal stability (up to temperatures higher than 200 °C), then the main decomposition process takes place, as follows: in the case of mixture with Sta, between 274 and 351 °C (DTG_{peak} at 316 °C), for PVP K30 between 287 and 346 °C (DTG_{peak} at 325 °C), for SiO_2 between 300 and 327 °C (DTG_{peak} at 316 °C), Talc between 300 and 341 °C (DTG_{peak} at 319 °C), Man between 280 and 354 °C (DTG_{peaks} at 331 and 340 °C) and MgSt between 285 and 354 °C (DTG_{peak} at 338 °C).

For the mixture of ABZ-RAMEB with excipients, a similar thermal profile to the one recorded for ABZ-HPBCD is reported (Fig. 9b, d). These samples also show a mass loss below 50 °C, due to dehydration, followed by a

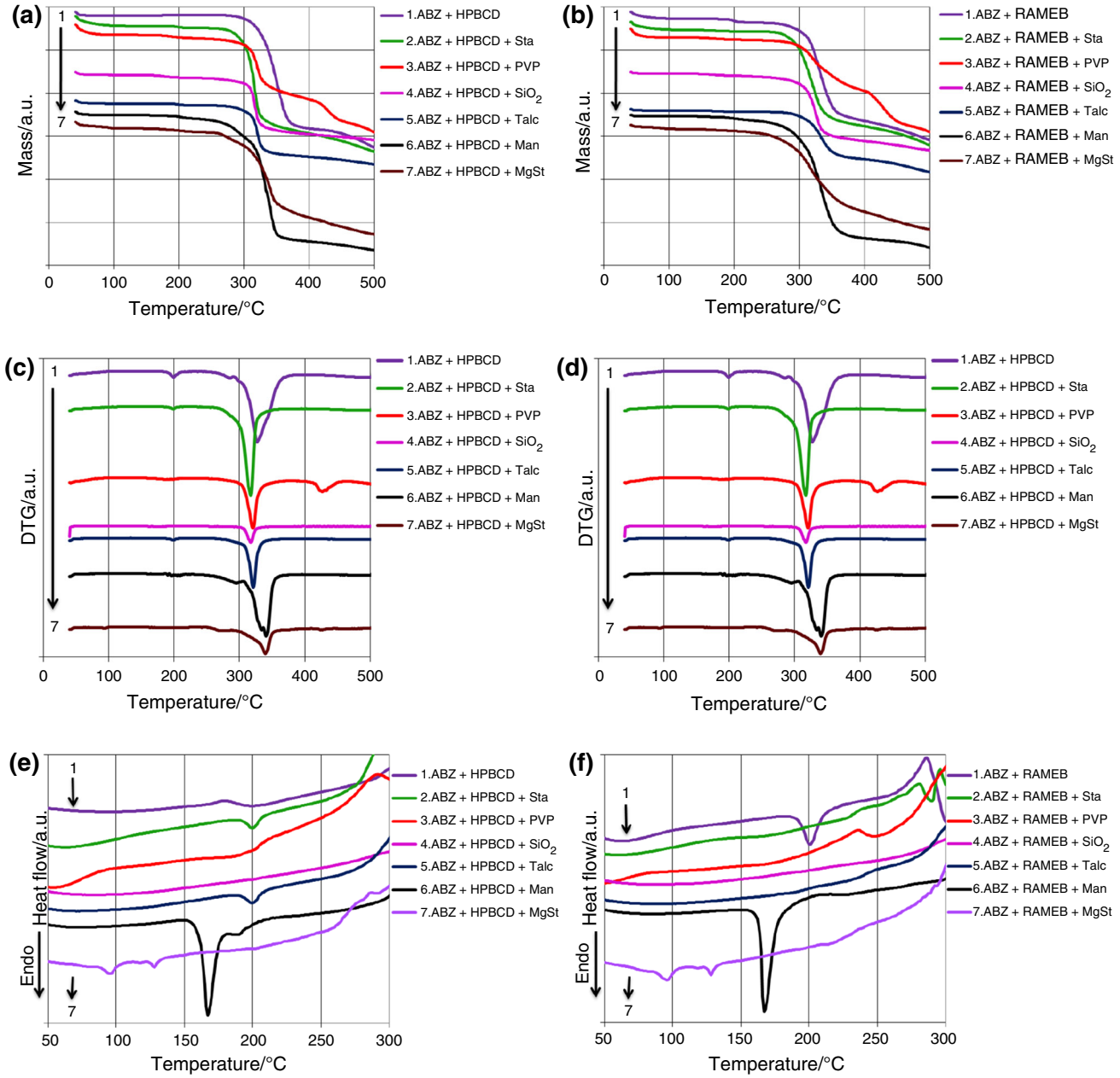

Fig. 9 Thermoanalytical curves obtained in air at 10 °C min^{-1} for binary mixtures of complexes with excipients for ABZ-HPBCD: **a** TG, **c** DTG, **e** HF and ABZ-RAMEB: **b** TG, **d** DTG, **f** HF

good thermal stability (up to temperatures higher than 200 °C), then the main decomposition process takes place, as follows: in the case of mixture with Sta, between 258 and 362 °C (DTG_{peak} at 313 °C), for PVP K30 between 271 and 375 °C (DTG_{peak} at 319 °C), for SiO_2 between 290 and 341 °C (DTG_{peak} at 322 °C), Talc between 279 and 369 °C (DTG_{peak} at 330 °C), Man between 253 and 389 °C (DTG_{peak} at 334 °C) and MgSt between 248 and 372 °C (DTG_{peak} at 310 °C).

As shown in Fig. 9e, f, the HF curves indicate the interactions of the complexes with excipients during thermolysis. In all cases, the HF profile of mixtures is different in comparison to the one of complexes, leading to the conclusion that interactions occur in all cases.

Conclusions

Our study evaluated the potential interactions between albendazole complexes with two modified cyclodextrins, HPBCD and RAMEB and various pharmaceutical excipients. The water solubility of the two semisynthetic cyclodextrins is significantly higher than the one of the native β-cyclodextrin which makes them more suitable carriers for pharmaceutical substances used in the biomedical field. The use of cyclodextrin complexes provides superior aqueous solubility to the active compound, subsequently increasing its bioavailability. In addition, toxicity studies showed a high safety profile for the two cyclodextrin derivatives used in the study.

Thermal analyses provided information about the thermal stability and decomposition of ABZ complexes and the binary mixtures with excipients, which gives valuable information for the quality control. In the DSC studies, the modifications found in the curves suggested a possible interaction of ABZ-HPBCD with PVP K30 and SiO_2 respectively, whereas in the case of ABZ-RAMEB + excipients, the DSC profiles suggested a physical interaction with talc. Finally, thermal analysis carried out in open crucibles in dynamic air atmosphere suggests that at temperatures over 40 °C dehydration of samples occurs, later followed by thermolysis and appearance of heated-induced interactions in all studied cases.

The events presented by DSC analysis are partially supported by the complementary techniques; the ATR-FTIR analysis clearly suggested interactions under ambient conditions between ABZ-HPBCD and SiO_2, ABZ-HPBCD and PVP K30, and between ABZ-RAMEB and talc, ABZ-RAMEB and SiO_2, respectively.

The PXRD patterns indicated the formation of less crystalline mixtures but with no clear indication of chemical interactions, since no peaks appeared nor disappeared. However, the modification of crystallinity should be evaluated, since it can affect the bioavailability of the API in the final formulations.

Following our study, precautions should be recommended in elaborating new solid formulations containing ABZ, HPBCD and PVP K30/SiO_2, respectively, and for the ones containing ABZ, RAMEB and Talc/SiO_2, since interactions have appeared under ambient conditions. It is worth mentioning that the interaction with SiO_2 was revealed under ambient conditions only by ATR-FTIR technique, in both types of complexes. The interaction with PVP K30 was found only for the ABZ-HPBCD complex and the one with Talc, only for the ABZ-RAMEB complex; these results were highlighted under ambient and thermal stress conditions.

These results offered a better understanding of the solid–solid interactions in multicomponent solid pharmaceutical formulations contributing to the rational design of novel materials.

Acknowledgements This work was supported by a grant financed by the University of Medicine and Pharmacy "Victor Babes" Timisoara (Grant PIII-C3-PCFI-2016/2017, acronym STONES to CT, IL and AL).

Author Contributions Conceived and designed the experiments: all authors. Performed the experiments: thermal analysis and ATR-FTIR spectroscopy: IL, AL, GV, FB; powder X-ray diffraction: ZA. Analyzed the data: all authors. Contributed reagents/materials/analysis tools: all authors. Wrote the paper: all authors

Compliance with ethical standards

Conflict of interest The authors declare no conflict of interest.

References

1. Evrard B, Chiap P, DeTullio P, Ghalmi F, Piel G, Van Hees T, Crommen J, Losson B, Delattre L. Oral bioavailability in sheep of albendazole from a suspension and from a solution containing hydroxypropyl-beta-cyclodextrin. J Control Release. 2002;85:45–50.
2. Pradines B, Gallard JF, Iorga B, Gueutin C, Loiseau PM, Ponchel G, Bouchemal K. Investigation of the complexation of albendazole with cyclodextrins for the design of new antiparasitic formulations. Carbohydr Res. 2014;398:50–5.
3. Codina AV, Garcia A, Leonardi D, Vasconi MD, Di Masso RJ, Lamas MC, Hinrichsen LI. Efficacy of albendazole:beta-cyclodextrin citrate in parenteral stage of *Trichinella spiralis* infections. Int J Biol Macromol. 2015;77:203–6.
4. Garcia A, Barrera MG, Piccirilli G, Vasconi MD, Di Masso RJ, Leonardi D, Hinrichsen LI, Lamas MC. Novel albendazole formulations given during the intestinal phase of *Trichinella spiralis* infection reduce effectively parasitic muscle burden in mice. Parasitol Int. 2013;62:568–70.
5. Pensel PE, Castro S, Allemandi D, Sanchez Bruni S, Palma SD, Ellisondo MC. Enhanced chemoprophylactic and clinical efficacy of albendazole formulated as solid dispersions in experimental cystic echinococcosis. Vet Parasitol. 2014;203:80–6.
6. Fromming KH, Szejtli J. Cyclodextrins in pharmacy. Dordrecht: Kluwer Academic Publishers; 1994.
7. Kata M, Schauer M. Increasing the solubility characteristics of albendazole with dimethyl-beta-cyclodextrin. Acta Pharm Hun. 1991;61:23–31.
8. Ghosh I, Nau WM. The strategic use of supramolecular pKa shifts to enhance the bioavailability of drugs. Adv Drug Deliv Rev. 2012;64:764–83.
9. Muankaew C, Jansook P, Stefánsson E, Loftsson T. Effect of gamma-cyclodextrin on solubilization and complexation of irbesartan: influence of pH and excipients. Int J Pharm. 2014;474:80–90.
10. Orgovan G, Kelemen H, Noszal B. Protonation and beta-cyclodextrin formation equilibria of fluconazole. J Incl Phenom Macrocycl Chem. 2016;84:189–96.
11. Kelemen H, Csillag A, Hancu G, Szekely-Szentmiklosi B, Fulop I, Varga E, Grama L, Orgovan G. Characterization of inclusion

complexes between bifonazole and different cyclodextrins in solid and solution state. Maced J Chem En. 2017;36:81–91.
12. Trandafirescu C, Gyéresi A, Kata M, Aigner Z, Szabadai Z. Interaction study of albendazole with hydroxypropyl-beta-cyclodextrin. Farmacia. 2006;5:86–94.
13. Trandafirescu C, Gyéresi A, Kata M, Aigner Z, Szabadai Z. Preparation and characterization of albendazole-random methyl-beta-cyclodextrin binary systems. Farmacia. 2007;1:98–107.
14. Trandafirescu C, Gyéresi A, Kata M, Aigner Z, Szabadai Z. Study of albendazole hydroxypropyl-beta-cyclodextrin binary systems. Farmacia. 2007;5:580–9.
15. di Cagno MP. The potential of cyclodextrins as novel active pharmaceutical ingredients. A short overview. Molecules. 2017;22:1. https://doi.org/10.3390/molecules22010001.
16. Peres-Filho MJ, Pedroso Nogueira Gaeti M, Ramirez de Oliveira S, Neves Mareto R, Martins Lima E. Thermoanalytical investigation of olanzapine compatibility with excipients used in solid oral dosage forms. J Therm Anal Calorim. 2011;104:255–60.
17. Yoshida MI, Oliveira MA, Gomes ECL, Mussel WN, Castro WV, Soares CDV. Thermal characterization of lovastatin in pharmaceutical formulations. J Thermal Anal Calorim. 2011;106:657–64.
18. Júlio T, Zâmara IF, Garcia JS, Trevisan MG. Compatibility of sildenafil citrate and pharmaceutical excipients by thermal analysis and LC-UV. J Therm Anal Calorim. 2013;111:2037–44.
19. Gao R, Sun B-W, Lin J, Gao X-L. Compatibility of medroxyprogesterone acetate and pharmaceutical excipients through thermal and spectroscopic techniques. J Therm Anal Calorim. 2014;117:731–9.
20. Shantikumar S, Sreekanth G, Surendra Nath KV, Jafer Valli S, Satheeshkumar N. Compatibility study between sitagliptin and pharmaceutical excipients used in solid dosage forms. J Therm Anal Calorim. 2014;115:2423–8.
21. Veronez IP, Daniel JSP, Garcia JS, Trevisan MG. Characterization and compatibility study of desloratadine. J Thermal Anal Calorim. 2014;115:2407–14.
22. Silva DLA, Vieira Teixeira F, Caixeta Serpa R, Locatelli Esteves N, dos Santos RR, Martins Lima E, Soares da Cunha-Filho MS, de Souza Antunes, Araújo A, Taveira SF, Neves Mareto R. Evaluation of carvedilol compatibility with lipid excipients for the development of lipid-based drug delivery systems. J Therm Anal Calorim. 2016;123:2337–44.
23. Pires SA, Mussel WN, Yoshida MI. Solid-state characterization and pharmaceutical compatibility between citalopram and excipients using thermal and non-thermal techniques. J Therm Anal Calorim. 2017;127:535–42.
24. Elder DP, Kuentz M, Holm R. Pharmaceutical excipients—quality, regulatory and biopharmaceutical considerations. Eur J Pharm Sci. 2016;87:88–9.
25. Nishath F, Mamatha T, Qureshi HK, Nandagopal A, Rao JV. Drug-excipient interaction and its importance in dosage form development. J Appl Pharm Sci. 2011;6:66–71.
26. Patel P, Ahir K, Patel V, Manani L, Patel C. Drug-excipient compatibility studies: first step for dosage form development. Pharma Innov. 2015;4:14–20.
27. Ledeti A, Vlase G, Vlase T, Bercean V, Murariu MS, Ledeti I, Suta L-M. Solid state preformulation on studies of amiodarone hydrochloride. J Therm Anal Calorim. 2016;126:181–7.
28. Ledeti I, Bolintineanu S, Vlase G, Circioban D, Dehelean C, Suta L-M, Caunii A, Ledeti A, Vlase T, Murariu M. Evaluation of solid-state thermal stability of donepezil in binary mixtures with excipients using instrumental techniques. J Therm Anal Calorim. 2017;130:425–31. https://doi.org/10.1007/s10973-017-6250-3.
29. Gohel MC, Patel TM. Compatibility study of quetiapine fumarate with widely used sustained release excipients. J Therm Anal Calorim. 2013;111:2103–8.
30. Chadha R, Bhandari S. Drug-excipient compatibility screening—Role of thermoanalytical and spectroscopic techniques. J Pharm Biomed Anal. 2014;87:82–97.
31. Pereira MAV, Fonseca GD, Silva-Júnior AA, Fernandes-Pedrosa MF, de Moura MDF, Barbosa EG, Gomes APB, dos Santos KSCR. Compatibility study between chitosan and pharmaceutical excipients used in solid dosage forms. J Therm Anal Calorim. 2014;116:1091–100.
32. Trandafirescu C, Soica C, Ledeti A, Borcan F, Suta L-M, Murariu M, Dehelean C, Ionescu D, Ledeti I. Preformulation studies for albendazole A DSC and FTIR analysis of binary systems with excipients. Rev Chim. 2016;67:463–7.
33. Crowley P, Martini LG. Drug-excipient interactions. Pharm Technol. 2001;13:26–34.
34. Duncan WB, O'Hare D. Inorganic Materials. 2nd ed. Hoboken: John Wiley & Sons; 1997.
35. Kiss D, Zelko R, Novak CS, Ehen ZS. Application of DSC and NIRS to study the compatibility of metronidazole with different pharmaceutical excipients. J Thermal Anal Calorim. 2006;84:447–51.
36. Borba PAA, Vecchia DD, Kluppel Riekes M, Pereira RN, Piazzon Tagliari M, Segatto Silva MA, Cuffini SL, Maduro de Campos CE, Stulzer HK. Pharmaceutical approaches involving carvedilol characterization compatibility with different excipients and kinetic studies. J Therm Anal Calorim. 2014;115:2507–15.
37. Ledeti I, Vlase G, Vlase T, Fulias A, Suta L-M. Comparative thermal stability of two similar-structure hypolipidemic agents. J Therm Anal Calorim. 2016;125:769–75.
38. Kumar N, Goindi S, Saini B, Bansal G. Thermal characterization and compatibility studies of itraconazole and excipients for development of solid lipid nanoparticles. J Therm Anal Calorim. 2014;115:2375–83.
39. https://pubchem.ncbi.nlm.nih.gov/compound/albendazole#section=NSC-Number.
40. https://www.chemsrc.com/en/searchResult/Randomly%20methylated-%CE%B2-Cyclodextrin/.
41. Ledeţi I, Murariu M, Vlase G, Vlase T, Doca N, Ledeţi A, Şuta L-M, Olariu T. Investigation of thermal-induced decomposition of iodoform. J Therm Anal Calorim. 2017;127(1):565–70.
42. Suta LM, Vlase G, Ledeti A, Vlase T, Matusz P, Trandafirescu C, Circioban D, Olariu S, Ivan C, Murariu MS, Stelea L, Ledeti I. Solid-state thermal behaviour of cholic acid. Rev Chim. 2016;67(2):329–31.
43. Ledeti A, Olariu T, Caunii A, Vlase G, Circioban D, Baul B, Ledeti I, Vlase T, Murariu M. Evaluation of thermal stability and kinetic of degradation for levodopa in non-isothermal conditions. J Therm Anal Calorim. 2017;131(2):1881–8.
44. Suta LM, Matusz P, Ledeti A, Ivan C, Murariu M, Sora MC, Ledeti I. Embedding of Biliary Calculi in Plastic Materials A viable solution for increasing their mechanical resistance during sampling. Mater Plast. 2016;53(1):19–22.
45. Ledeti A, Vlase G, Vlase T, Bercean V, Murariu MS, Ledeti I, Suta LM. Solid-state preformulation studies of amiodarone hydrochloride. J Therm Anal Calorim. 2016;126(1):181–7.

Affiliations

Cristina Trandafirescu[1] · Ionuţ Ledeţi[1] · Codruţa Şoica[1] · Adriana Ledeţi[1] · Gabriela Vlase[2] · Florin Borcan[1] · Cristina Dehelean[1] · Dorina Coricovac[1] · Roxana Racoviceanu[1] · Zoltán Aigner[3]

[1] Department of Pharmaceutical Chemistry, Faculty of Pharmacy, "Victor Babeş" University of Medicine and Pharmacy, 2nd Eftimie Murgu Square, 300041 Timisoara, Romania

[2] Research Centre for Thermal Analysis in Environmental Problems, West University of Timişoara, 16th Pestalozzi Street, 300115 Timisoara, Romania

[3] Institute of Pharmaceutical Technology and Regulatory Affairs, University of Szeged, 6th Eötvos Street, Szeged 6720, Hungary